[Chem. Pharm. Bull. 27(7)1626—1635(1979)]

UDC 546.17'27.02.03 : 541.5.04

Energy Decomposition Analysis of Borazane at the Molecular Orbital Level: Origin of the Internal Rotation Barrier of H_3X-YH_3

HIDEAKI UMEYAMA[1a] and TAKAO MATSUZAKI[1b]

School of Pharmaceutical Sciences, Kitasato University[1a] and Central Research Laboratories, Mitsubishi Chemical Industries Ltd.[1b]

(Received January 31, 1979)

The origin of the borazane complex, which is composed of $NH_3(C_{3v})$ and $BH_3(C_{3v})$, was studied from a quantum-chemical point of view. Calculations were carried out by the *ab initio* method. A double zeta basis set with polarization functions (4-31G**) and a single zeta basis set (STO-3G) were used. In order to identify the origin of the complex, energy decomposition analyses were carried out at the molecular orbital level. Among the MO–MO interactions which contribute to charge transfer (CT) in the complex formation, the following are significant in the order indicated.

$$CT_{H_3N,3a_1\to BH_3,3a_1} > CT_{H_3N,3a_1\to BH_3,5a_1} > CT_{H_3N,5a_1\leftarrow BH_3,2a_1} > CT_{H_3N,2e\leftarrow BH_3,1e}$$

As for the repulsion energy, A_1–A_1 and valence-valence MO interactions were significant. HOMO–HOMO interaction was dominant in exchange repulsion. Moreover, valence-core MO interaction and E–E MO interaction could not be neglected.

On the other hand, it appeared that the internal rotation barrier of the complex might originate from le–le MO interaction. Therefore the same analysis was applied to ethane, disilane, methylsilane, H_3B–CH_3^- and H_3N–CH_3^+. These quantitative analyses showed that the le–le MO interaction is the most important component in the internal rotation barrier of these compounds and complexes.

Keywords——rotation barrier; borazane; molecular complex; molecular orbital; ammonia complex; boron complex; ethane; energy decomposition; structure; MO

Fujimoto *et al.* studied the origin of the charge transfer and bond formation between boron hydride and ammonia in borazane complex, expanding the Slater AO into three Gaussian functions.[2] They reported that HOMO of NH_3 and LUMO of BH_3 are significant in the chemical interaction based on estimation of the electron occupation number of isolated molecules, and configuration analyses, including the charge transfer and polarized states. Umeyama and Morokuma then performed energy decomposition analysis, force decomposition analysis, and charge decomposition analysis using a 4-31G basis set.[3] The origin of the interaction energy of the borazane was electrostatic energy and charge transfer energy. The interaction force originated from electrostatic force (56%), charge transfer force (24%), and polarization force (20%). The borazane complex thus appears to belong to the class of "charge controlled" complexes.

In this paper, the following points were studied.

(1) Although the electrostatic interaction energy (69%) was larger than the charge transfer energy (20%) according to the paper by Umeyama and Morokuma,[3] calculations with a 4-31G basis set[4] usually overestimate electrostatic interaction energy due to overestimated dipole moment.[5] In order to confirm the "charge controlled" interactions assigned to borazane, calculations (4-31G**)[6] including *d*-orbitals on carbon and boron atoms and

1) Location: *a) 5-9-1, Shirokane Minato-ku, Tokyo 108, Japan; b) Kamoshida, Midori-ku, Yokohama 227, Japan.*
2) Y. Fujimoto, S. Kato, S. Yamabe, and K. Fukui, *J. Chem. Phys.*, **60**, 572 (1974).
3) H. Umeyama and K. Morokuma, *J. Am. Chem. Soc.*, **98**, 7208 (1976).
4) R. Ditchfield, W.J. Hehre, and J.A. Pople, *J. Chem. Phys.*, **54**, 724 (1971).
5) H. Umeyama and K. Morokuma, *J. Am. Chem. Soc.*, **99**, 1316 (1977).
6) P.C. Hariharan and J.A. Pople, *Theor. Chim. Acta*, **28**, 213 (1973).

p-orbitals on hydrogens were carried out. In the calculations for HF–ClF complex and H_2O dimer the usefulness of the polarization functions has already been shown.[7]

(2) The wave function of the complex can be written by using a combination of various electron configurations, including charge transfer and polarized states, as follows:[2]

$$\Psi = C_0\Psi_0 + (\sum_{p}^{ct} C_p\Psi_p + \sum_{q}^{dict} C_q\Psi_q + \sum_{r}^{pl} C_r\Psi_r + \cdots\cdots)$$

where Ψ_0 is the state in which neither electron transfer nor electron excitation takes place, ct means a single electron transfer configuration, dict implies transfer of two electrons, pl denotes a locally excited configuration of a single electron in one of the two reactants. In the equation the coefficients correspond to the contributions of the states to the complex. However, the contributions are not quantitatively known. In this report, the contribution of the unoccupied MO's in the charge transfer process is quantitatively described by analysis of the intermolecular charge transfer MO interactions.

(3) The rotational barrier between the eclipsed and staggered structures of borazane was explained by the difference of exchange repulsion.[3] In order to identify the origin of the exchange repulsion, energy decomposition analysis at the MO level was carried out.

(4) The method used in (3) was applied to identify the origin of the internal rotation barrier of the H_3X–YH_3 molecule.

Method

All calculations were performed within the framework of a closed-shell single determinant of the *ab initio* LCAO MO–SCF theory, using the GAUSSIAN 70 program.[8] The split-valence 4-31G basis set was used with the suggested standard scale factors.[4] This set has a tendency to overestimate the polarity of the isolated molecules.[5] This is reflected in an exaggerated dipole moment, and consequently in an overestimated electrostatic interaction. Therefore, the larger 4-31G** basis set which includes one set of polarization functions on each atom (p function with the exponent $\alpha=1.1$ for a hydrogen atom and d function with $\alpha=0.8$ for other atoms) was used. The IBMOLH program has been used for evaluation of the integrals for the 4-31G** set.

Energy decomposition analysis was performed by the method of Kitaura and Morokuma.[9] The mechanics of the calculations of energy and charge distribution components have been summarized in the paper of Umeyama and Morokuma.[3] The interaction energies at the MO level between A_1 symmetry MO's and E symmetry MO's set were calculated by the generalized method of Umeyama and Morokuma.[5] A_1 MO's are σ MO's, and E MO's are π MO's.

ΔE is the interaction energy in the complex formation, and can be divided as follows.

$$\Delta E = ES + EX + PL + CT + MIX,$$

Where ES is electrostatic energy, EX is exchange repulsion, PL is polarization energy, CT is charge transfer energy and MIX is coupling energy. EX was separated into two parts, X+EX′.

$$EX = X + EX'$$

Where $X(-\sum K)$ is an attractive contribution of exchange integrals, and EX′ (overlap) the repulsive contribution of the overlap integrals.

When $\Delta\rho$ is the total electron density change on atoms,

$$\Delta\rho = \rho_{EX} + \rho_{PL} + \rho_{CT+MIX}$$

where ρ_{EX} is the change due to EX, ρ_{PL} is due to PL, and ρ_{CT+MIX} is due to CT+MIX.

The relative magnitude of CT from the electron donor ED to the electron acceptor EA and that from EA to ED is of interest with regard to the nature and origin of the electron

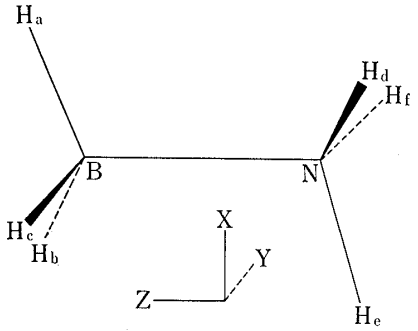

Fig. 1. Structure of the Borazane Complex

7) H. Umeyama, K. Morokuma, and S. Yamabe, *J. Am. Chem. Soc.*, **99**, 330 (1977).
8) W.J. Hehre, W.A. Lathan, R. Ditchfield, M.D. Newton, and J.A. Pople, "Quantum Chemistry Program Exchange," Indiana University, U.S.A., 1973.
9) K. Kitaura and K. Morokuma, *Int. J. Quantum Chem.*, **10**, 325 (1976).

donor-acceptor (EAD) complex. If $CT_{H_3N\rightarrow BH_3}$ is the charge transfer energy from NH_3 to the BH_3 molecule, the difference between CT and $CT_{H_3N\rightarrow BH_3}+CT_{H_3N\leftarrow BH_3}$ is called the coupling term CT_{MIX},

$$CT = CT_{H_3N\rightarrow BH_3} + CT_{H_3N\leftarrow BH_3} + CT_{MIX}$$

Another method of dividing the CT interaction is to consider CT between the MO's with irreducible representation A_1 ($ED_{A_1}\rightarrow EA_{A_1}$* and $EA_{A_1}\rightarrow ED_{A_1}$*) and CT between the MO's with irreducible representation E ($ED_E\rightarrow EA_E$* and $EA_E\rightarrow ED_E$*) separately. A_1 MO's are symmetric with respect to the B–N bond axis as shown in Figure 1, and these MO's are not degenerate. Degenerate E MO's of the isolated molecules, NH_3 and BH_3, are transformed to symmetric and antisymmetric MO's with respect to the xz plane by the operations, $1/\sqrt{2}(\Psi_1+\Psi_2)$ and $1/\sqrt{2}(\Psi_1-\Psi_2)$.

Monomer Geometries——In the calculations, it is assumed that the geometry of the isolated electron donor, NH_3, is not altered upon complex formation. The geometry of $NH_3(C_{3v})$ is $r(NH)=1.0124$ Å and $<HNH=106.67°$.[5] For BH_3, a single geometry was studied: a pyramidal (C_{3v}) configuration, which is the expected conformation in the complexed form. The geometry is $r(BH)=1.19$ Å and $<HBZ=106.3°$ (Z is the C_{3v} axis).[3] The distance between B and N is optimized at 1.70492 Å.[3] For the structure of ethane, the experimental values were used.[11] For disilane and methylsilane, the geometries were obtained from the table by Sutton.[10] For $H_3N–CH^+_3$ and $H_3B–CH^-_3$, the NH_3 and BH_3 parts are the same as in $H_3N–BH_3$, and the CH^+_3 and CH^-_3 parts are the same as those of ethane. The distance between C and N is 1.474 Å, which is that found in CH_3NH_2, and the distance between B and C is 1.56 Å, which is the value in $(CH_3)_3B$.

In calculations of the rotational barrier, the rigid-rotor approximation was applied.[3] Calculations were carried out using a HITAC 8700 and 8800 machines in the Tokyo University Computer Center and an IBM 370-158 in Mitsubishi Chemical Industries Ltd.[12]

Results

MO levels of $BH_3(C_{3v})$ and $NH_3(C_{3v})$ including polarization functions in a basis set are shown in Table I together with the results obtained using a 4-31G basis set. MO levels with both the 4-31G and 4-31G** basis sets are very similar. The total electron densities of the isolated molecules are shown in Table II. In comparison with the results using a 4-31G basis set, the total electron densities of nitrogen and boron obtained using 4-31G** decreased. On the other hand those of hydrogens in BH_3 and NH_3 increased. Thus, by including the polarization functions, the electrons in NH_3 are moved from the nitrogen to the hydrogens, and the electrons in BH_3 are moved from the boron to the hydrogens. The changes of

Table I. MO Levels in a. u. of the BH_3 (C_{3v}) and NH_3 (C_{3v}) Parts Using 4-31G and 4-31G** Basis Sets

NH_3			BH_3		
MO	4-31G	4-31G**	MO	4-31G	4-31G**
4e	1.287	1.200	4e	1.239	1.171
$6a_1$	1.246	1.160	$6a_1$	0.912	0.890
$5a_1$	1.060	1.040	$5a_1$	0.747	0.747
3e	0.974	0.930	3e	0.670	0.661
2e	0.323	0.326	$4a_1$	0.324	0.327
$4a_1$	0.221	0.227	2e	0.318	0.320
			$3a_1$	0.070	0.072
$3a_1$	−0.414	−0.419	1e	−0.483	−0.483
1e	−0.623	−0.618	$2a_1$	−0.709	−0.706
$2a_1$	−1.145	−1.132	$1a_1$	−7.601	−7.597
$1a_1$	−15.509	−15.517			

10) E. Sutton, "Tables of Interatomic Distances and Configuration in Molecules and Ions," The Chemical Society, London, 1958.
11) G. Herzberg, "Electronic Spectra of Polyatomic Molecules," Van Nostrand Reinhold, New York, N.Y., 1968.
12) The IBM computer was used in calculations including polarization functions.

Table II. Change of Components of Gross Population in the Complex H_3N–BH_3; C_{3v} Approach at r (N···B)=1.705 Å Using a 4–31G** Basis Set

	a)	ρ_{EX}	ρ_{PL}	ρ_{CT+MIX}	$\Delta\rho$
			4-31G*b*)		
H	0.702	0.003	−0.086	0.001	−0.082
N	7.894	−0.010	0.257	−0.188	0.059
B	4.807	−0.042	−0.062	0.036	−0.067
H	1.064	0.014	0.021	0.050	0.085
BH_3		0.0	0.0	0.187	0.187
			4-31G**		
H	0.755	0.003	−0.080	0.010	−0.067
N	7.736	−0.010	0.239	−0.257	−0.028
B	4.712	−0.039	−0.032	0.030	−0.041
H	1.096	0.013	0.011	0.066	0.090
BH_3		0.0	0.0	0.229	0.229

Positive and negative values indicate an increase and a decrease, respectively, of electron population upon complex formation. The sum of the atoms is BH_3. The sums for NH_3 are negatives of the BH_3 values.
a) Total electron densities from the data for the two isolated molecules.
b) Reference 3.

components of gross populations in the complex are shown in Table II. The exchange repulsion decreases the populations of N and B, and it increases those of the hydrogens of NH_3 and BH_3. The population changes were larger in BH_3 than in NH_3. Because of the effects polarization functions, the electrons are moved from the hydrogens to N in NH_3, and from B to the hydrogens in BH_3. Due to the charge transfer and coupling effects, the electrons are moved from NH_3 to BH_3. In total, the populations of NH_3 and B decrease due to the intermolecular interaction, and those of the hydrogens in BH_3 increase. The calculations with the polarization functions gave larger $\Delta\rho$ and ρ_{CT+MIX} of BH_3, and smaller ρ_{EX} and ρ_{PL}.

Table III shows the results of the energy decomposition calculations. The interaction energy was 40.9 kcal/mol. The stabilization energy originated from electrostatic (60.6%), charge transfer (21.9%), and polarization (17.5%) energies. Therefore the dominant contributor to the stabilization was the electrostatic interaction energy. This result was in agreement with that using a 4-31G basis set.[3] The interaction energy using 4-31G** was smaller than

Table III. Interaction Energy and Energy Decomposition Analysis in kcal/mol of Borazane at r (N···B)=1.705 Å Using a 4–31G** Basis Set

	4–31G*a*)	4–31G**	Difference
ΔE	−44.7	−40.9	3.8
ES	−92.9	−81.2	11.7
EX	86.9	85.9	−1.0
(Overlap)	(187.2)	(180.1)	(−7.1)
$(-\sum K)$	(−100.3)	(−94.2)	(6.1)
PL	−17.2	−23.5	−6.3
CT	−27.1	−29.3	−2.2
$CT_{H_3N\rightarrow BH_3}$	−19.4	−21.6	−2.2
$CT_{H_3N\leftarrow BH_3}$	−7.4	−7.4	0.0
CT_{MIX}	−0.3	−0.3	0.0
MIX	5.6	7.3	1.7

a) Reference 3.

that using 4-31G by 3.8 kcal/mol; this destabilization was mainly due to the difference in ES. Since the 4-31G calculations overestimate ES, the ES term will be most affected. It should be noted that PL was increased by inclusion of the polarization functions by 6.3 kcal/mol. This confirms the significance of the polarization functions for the interaction energy of the complex. CT was increased by 2.2 kcal/mol with the inclusion of polarization functions; the contribution of the polarization functions to CT was thus rather small. CT, $CT_{H_3N\rightarrow BH_3}$, and $CT_{H_3N\leftarrow BH_3}$ are shown in Table III. CT_{MIX} and $CT_{H_3N\leftarrow BH_3}$ using 4–31G** are the same as those obtained using 4-31G. On the other hand $CT_{H_3N\rightarrow BH_3}$ increases by 2.2 kcal/mol in a similar comparison. The ratio $CT_{H_3N\rightarrow BH_3}/CT_{H_3N\leftarrow BH_3}$ was 2.9. This value shows that the charge transfer from NH_3 to BH_3 is three times larger than that from BH_3 to NH_3. That is, $CT_{H_3N\rightarrow BH_3}$ was 74% of CT.

Among the charge transfer components from NH_3 to BH_3, CT through A_1 MO's ($CT_{H_3N,A_1\rightarrow BH_3,A_1}$) and that through E MO's accounted for 95% and 5%, respectively, as shown in Table IV. The CT coupling between A_1 MO's and E MO's was zero. Among the charge

Table IV. Energy Decomposition Analysis in kcal/mol of CT and EX′ at the MO Level for Borazane Complex Using a 4–31G** Basis Set

		NH_3	BH_3	CT	Referred term	Ratio %
(1)	$\rightleftharpoons$	A_1+E	A_1+E	−29.3		
(2)	$\rightarrow$	A_1+E	A_1+E	−21.6	(2) + (3)	74
(3)	$\leftarrow$	A_1+E	A_1+E	−7.4	(2) + (3)	26
(4)	$\rightarrow$	A_1	A_1	−20.6	(4) + (5)	95
(5)	$\rightarrow$	E	E	−1.0	(4) + (5)	5
(6)	$\leftarrow$	A_1	A_1	−4.9	(6) + (7)	66
(7)	$\leftarrow$	E	E	−2.5	(6) + (7)	34
(8)	$\rightarrow$	$3a_1$	$3a_1$	−17.8	(3)	86
(9)	$\rightarrow$	$3a_1$	$4a_1$	−0.2	(3)	1
(10)	$\rightarrow$	$3a_1$	$5a_1$	−7.6	(3)	37
(11)	$\leftarrow$	$4a_1$	$2a_1$	−0.1	(6)	2
(12)	$\leftarrow$	$5a_1$	$2a_1$	−3.9	(6)	81
(13)	$\leftarrow$	2e	1e	−1.3	(7)	53
(14)	$\leftarrow$	3e	1e	−0.1	(7)	3
(15)	$\leftarrow$	4e	1e	−0.5	(7)	20

	NH_3	BH_3	EX′	Referred term	Ratio %
(16)	A_1+E	A_1+E	180.1		
(17)	A_1	A_1	154.2	(17) + (18)	85
(18)	E (1e)	E (1e)	27.0	(17) + (18)	15
(19)	A_1 valence ($2a_1$ and $3a_1$)	A_1 valence ($2a_1$)	112.8	(19) + (20) + (21) + (22)	75
				(16)	63
(20)	A_1 core ($1a_1$)	A_1 core ($1a_1$)	0.0	(19) + (20) + (21) + (22)	0
(21)	A_1 valence ($2a_1$ and $3a_1$)	A_1 core ($1a_1$)	34.1	(19) + (20) + (21) + (22)	23
				(16)	19
				(21) + (22)	90
(22)	A_1 core ($1a_1$)	A_1 valence ($2a_1$)	3.6	(19) + (20) + (21) + (22)	2
				(21) + (22)	10
(23)	$2a_1$	$2a_1$	30.1	(19)	27
(24)	$3a_1$ (HOMO)	$2a_1$ (HOMO)	87.9	(19)	78
				(16)	49

transfer components from BH_3 to NH_3, CT through A_1 MO's and that through E MO's accounted for 66% and 34%, respectively. The CT coupling between A_1 MO's and E MO's was −0.1 kcal/mol. Since $CT_{H_3N,A_1\to BH_3,A_1}$ was 95% of $CT_{H_3N\to BH_3}$, this term was analyzed at the MO level. $CT_{H_3N,3a_1\to BH_3,3a_1}$ was the largest contributor (86%). $CT_{H_3N,3a_1\to BH_3,5a_1}$ was the second largest (37%). In $CT_{H_3N,A_1\leftarrow BH_3,A_1}$, $CT_{H_3N,5a_1\leftarrow BH_3,2a_1}$ was the largest contributor (81%). In $CT_{H_3N,E\leftarrow BH_3,E}$, $CT_{H_3N,2e\leftarrow BH_3,1e}$ was 53%, and $CT_{H_3N,4e\leftarrow BH_3,1e}$ was the second largest (20%). The order in MO–MO interactions contributing to CT was $CT_{H_3N,3a_1\to BH_3,3a_1} > CT_{H_3N,3a_1\to BH_3,5a_1} > CT_{H_3N,5a_1\leftarrow BH_3,2a_1} > CT_{H_3N,2e\leftarrow BH_3,1e}$. Thus the contribution of MO–MO interaction to CT was clarified.

EX′ was separated into E and A_1 contributions. EX'_{H_3N,A_1-BH_3,A_1} and $EX'_{H_3N,E-BH_3,E}$ were 85% and 15%, respectively. Although the repulsion energy between the two A_1 MO's sets is dominant, the repulsion energy between the two E MO's sets cannot be neglected. The repulsion energy between valence and valence MO's sets was 75% in A_1 MO's sets and 63% in EX′. In EX′ the repulsion energy between valence and core (ls) MO's sets was 25%, of which 90% was $EX'_{H_3N,\text{valence}-BH_3,\text{core}}$. Since the repulsion energy between the valence MO's set in NH_3 and the core MO in BH_3 was 19% in EX′, the valence-core repulsion energy is significant. The repulsion energy between core and core MO's in both molecules was zero.

$EX'_{H_3N,\text{HOMO}-BH_3,\text{HOMO}}$ constituted 78% of EX'_{H_3N,A_1-BH_3,A_1} and 49% of EX′. The contribution of HOMO–HOMO interaction was large. Accordingly, A_1–A_1 MO interaction and valence-valence MO interaction were significant. HOMO–HOMO interaction was dominant in these interactions. The valence-core MO interaction and E–E MO interaction could not be neglected.

TABLE V. Energy Decomposition of the Rotational Barrier in kcal/mol for H_3N–BH_3 at r (N···B) = 1.705 Å Using an STO-3G Basis Set

	Staggered	Eclipsed	Difference	Results from 4–31G
ΔE	−64.5	−62.9	1.6	1.5
ES	−57.9	−58.1	−0.2	−0.3
EX	58.0	59.5	1.5	1.6
(Overlap)	115.1	117.6	(2.5)	(2.9)
$(-\sum K)$	−57.1	−58.1	(−1.0)	(−1.3)
PL	−2.0	−2.1	−0.0	−0.1
CT	−38.7	−38.0	0.6	0.6
MIX	−23.9	−24.2	−0.3	−0.3

H_3N	BH_3	EX′ (Overlap)		
		Staggered	Eclipsed	Difference
1e	1e	20.6	23.2	2.5
$2a_1$	$2a_1$	24.0	24.2	0.2
$3a_1$	$2a_1$	58.6	58.4	−0.2
$2a_1$ and $3a_1$	$2a_1$	79.4	79.4	−0.0
$2a_1$ and $3a_1$	$1a_1$	12.2	12.2	0.0
$1e_\pi$	$1e_\pi$	10.3	11.6	1.3
$1e_{\pi'}$	$1e_{\pi'}$	10.3	11.6	1.3

$1e_\pi$ of NH_3: $2p_x = 0.593$, $H_d = H_f = -2H_e = 0.248$.
$1e_\pi$ of BH_3: $2p_x = -0.515$, $-2H_a = H_b = H_c = 0.261$.
$1e_{\pi'}$ of NH_3: $2p_y = -0.515$, $H_a = 0$, $H_b = -H_c = -0.451$.
$1e_{\pi'}$ of BH_3: $2p_y = -0.593$, $H_e = 0$, $H_d = -H_f = 0.429$.

Energy Decomposition of the Rotational Barrier at the MO Level

Umeyama and Morokuma reported that the rotational barrier of borazane is essentially caused by the difference of overlap integrals in exchange repulsion.[13] In this study energy decomposition of the rotational barrier was performed at the MO level. The results are shown in Table V. The differences between the interaction energies of eclipsed and staggered structures correspond to the rotational barrier. Calculations were carried out using an STO-3G basis set, since the results obtained with an STO-3G basis set are in good agreement with those using a 4-31G basis set.[13] Calculations of the rotational barrier using an STO-3G basis set did not show basis set dependency. Next, EX′ was analyzed at the MO level. The results are also shown in Table V. $\Delta EX'_{H_3N,A_1\text{valence}-BH_3,\text{core}}$ $\Delta EX'_{H_3N,A_1\text{valence}-BH_3,A_1\text{valence}}$ were zero, where A_1 valence means σ MO's in valence MO's and core means an MO in which the coefficient of ls AO is large. Although these repulsion terms (greatly) contributed to EX′ of borazane complex formation, they are not the cause of the rotational barrier. The rotational barrier was attributed to $EX'_{H_3N,1e-BH_3,1e}$. That is, the repulsion energy between E irreducible representation MO's was the dominant contributor. Accordingly, the barrier is apparently caused by the orthogonality of intermolecular 1e–1e MO's that is required between BH and NH orbitals on opposite ends of the molecules. The BN bond does not participate significantly in the rotational barrier. Figure 2 shows E MO's of BH_3 and NH_3 in the staggered and eclipsed structures. Since E MO's are degenerate, two pairs are described. The repulsion energies of these pairs are also shown in Table V.

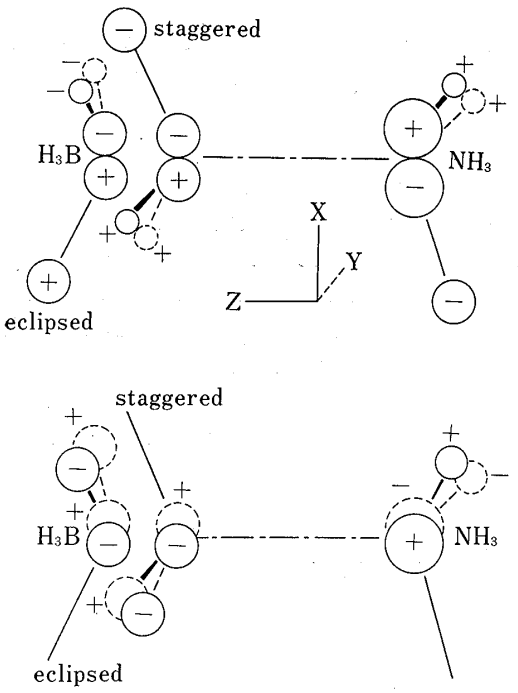

Fig. 2. E Symmetry Molecular Orbitals (Pseudo π MO's) of BH_3 and NH_3

Approach to the Rotational Barrier of Ethane

Morokuma and Umeyama reported, after analysis of the rotational barrier of borazane,[3] that the internal rotation barrier of ethane is determined in principle by the overlap terms of the exchange repulsion (EX′).[13] Moreover, they stated that the processes of the ion-ion interaction CH_3^+–CH_3^- and the radical-radical interaction $CH_3\cdot$–$CH_3\cdot$ both give the same results concerning the origin of the rotational barrier. The results using a 4-31G basis set were very similar to those using an STO-3G basis set in their paper. In our study, energy decomposition analysis of EX′ was performed at the MO level. Table VI shows the results. The overlap repulsion between le MO's was the dominant contributor. Sovers *et al.* concluded by using simple bond-orbital Hartree–Fock and Hartree product wave functions that the orbital orthogonality determines the rotational barrier of ethane.[14] Christiansen and Palke, using a partially antisymmetrized wave function (the valence-bond method),

$$\Psi = (A\phi_{1s_1}\phi_{1s_2}\phi_{CC})(A\phi_{CH_1}\phi_{CH_2}\phi_{CH_3})(A\phi_{CH_4}\phi_{CH_5}\phi_{CH_6})$$

reported that the orthogonality of CH orbitals on opposite ends of the molecule, which is required by the Pauli principle, causes the barrier.[15] Moreover, Morokuma and Umeyama,

13) K. Morokuma and H. Umeyama, *Chem. Phys. Letts.*, **49**, 333 (1977).
14) O.J. Sovers, C.W. Kern, R.M. Pitzer, and M. Karplus, *J. Chem. Phys.*, **49**, 2592 (1968).
15) P.A. Christiansen and W.E. Palke, *Chem. Phys. Letts.*, **31**, 462 (1975).

using the generalized energy decomposition method,[5] reported that the rotational barrier of ethane could be calculated by using the partially antisymmetrized MO wave function.[13]

$$\Psi = (A\phi_{CH_3^-})(A\phi_{CH_3^+}) \text{ or } (A\phi_{CH_3\cdot})(A\phi_{CH_3\cdot})$$

Since bonding or antibonding interaction between vicinal hydrogens is brought about by the need for orbital orthogonality and normality, Pople and Santry attributed the rotational barrier to the bonding-antibonding nature of vicinal hydrogen atoms in staggered ethane.[16] In Table VI of this paper, moreover, it was confirmed that 1e-1e in H_3C^-–CH_3^+ is quantitatively dominant as an MO interaction.

Table VI. Energy Decomposition of the Rotational Barrier in kcal/mol for Ethane at the MO Level Using an STO-3G Basis Set

CH_3^-	CH_3^+	Staggered	Eclipsed	Difference
1e	1e	37.8	42.3	4.6
$2a_1$	$2a_1$	39.8	40.2	0.4
$3a_1$	$2a_1$	174.1	173.8	−0.3
$1e_\pi$	$1e_\pi$	18.8	21.2	2.4
$1e_{\pi'}$	$1e_{\pi'}$	18.8	21.2	2.4

Rotational Barriers of H_3Si-SiH_3, H_3C-SiH_3, H_3N-CH_3^+, and H_3B-CH_3^-

The internal rotational barriers for H_3X–YH_3 molecules were next analyzed. Table VII shows the energy decomposition of the rotational barrier of disilane. The main contributor to the rotational barrier was exchange repulsion. Since the overlap term is dominant in EX, it was analyzed at the MO level. The MO interactions between valence pseudo π MO's of SiH_3^- and SiH_3^+ accounted for the overlap term. Since the conclusions from the molecular decompositions of ethane into CH_3^- and CH_3^+ and into $CH_3\cdot$ and $CH_3\cdot$ were the same, only the decomposition into SiH_3^- and SiH_3^+ was performed. Therefore the smaller separation between the localized pseudo π MO's in the opposite SiH bonds of the eclipsed form gave rise to a larger repulsion due to the orthogonality requirement than in the case of the staggered form.

Table VII. Energy Decomposition of the Rotational Barrier in kcal/mol for Disilane Using an STO-3G Basis Set

	Staggered	Eclipsed	Difference
ΔE	−372.80	−372.27	0.53
ES	−212.44	−212.32	0.11
EX	53.98	54.21	0.23
(Overlap)	(102.20)	(102.53)	(0.34)
$(-\sum K)$	(−48.21)	(−48.32)	(−0.11)
PL	−10.65	−10.62	0.03
CT	−133.82	−133.73	0.09
MIX	−69.88	−69.81	0.07

SiH_3^-	SiH_3^+	Staggered	Eclipsed	Difference
$4a_1$ and $5a_1$	$4a_1$	70.00	69.92	−0.08
2e	2e	3.25	3.67	0.43

16) J.A. Pople and D.P. Santry, *Mol. Phys.*, **9**, 301 (1965).

Table VIII. Energy Decomposition of the Rotational Barrier in kcal/mol for Methylsilane Using an STO-3G Basis Set

	$H_3C^- - SiH_3^+$			$H_3C^+ - SiH_3^-$		
	Staggered	Eclipsed	Difference	Staggered	Eclipsed	Difference
ΔE	−401.3	−400.0	1.3	−452.9	−451.7	1.3
ES	−300.1	−300.0	0.1	−252.4	−252.7	−0.2
EX	83.1	84.2	1.1	128.6	129.2	0.7
(Overlap)	(158.6)	(160.3)	(1.7)	(244.9)	(246.0)	(1.0)
$(-\sum K)$	(−75.4)	(−76.1)	(−0.6)	(−116.4)	(−116.7)	(−0.4)
PL	−20.6	−20.6	−0.0	−11.1	−11.0	0.1
CT	−79.2	−78.7	0.5	−143.1	−142.9	0.2
MIX	−84.6	−85.0	−0.4	−174.9	−174.4	0.5
a_1's—a_1's	88.8	88.8	0.0	20.5	20.6	0.1
e — e	13.4	15.2	1.7	11.4	12.6	1.3

In the combination between CH_3^- and SiH_3^+ the selected MO's are $2a_1$ and $3a_1$ for CH_3^- and $4a_1$ for SiH_3^+.

In the combination between CH_3^+ and SiH_3^-, the selected MO is $2a_1$ for CH_3^+ and $4a_1$ and $5a_1$ for SiH_3^-.

Table VIII shows the energy decomposition of the rotational barrier of methylsilane. Two molecular decompositions into CH_3^- and SiH_3^+ and into CH_3^+ and SiH_3^- were taken into account. In both cases, the main contributor to the exchange repulsion was EX. The overlap term contributed to EX. Analysis at the MO level showed the significance of the MO interactions between valence pseudo π MO's of the CH_3 and SiH_3 groups. Accordingly the conclusion for methylsilane was the same as for ethane and disilane.

Although experimental values are not available for H_3N–CH_3^+ and H_3B–CH_3^-, these rotational barriers were studied in order to confirm the conclusion that the internal rotation barrier of an H_3X–YH_3 type molecule originates from the MO interactions between pseudo π MO's localized in –XH and –YH bonds. Table IX and X shows these results. It is clear that the overlap term in EX is most significant, and it is attributed to the pseudo π MO's interactions between BH_3 and CH_3^-, and between NH_3 and CH_3^+.

Table IX. Energy Decomposition of the Rotational Barrier in kcal/mol for H_3N–CH_3^+ Using an STO-3G Basis Set

	Staggered	Eclipsed	Difference
ΔE	−171.1	−168.5	2.7
ES	−141.8	−141.9	−0.2
EX	139.2	141.5	2.3
(Overlap)	(266.3)	(270.2)	(3.9)
$(-\sum K)$	(−127.1)	(−128.6)	(−1.5)
PL	−10.2	−10.2	0.0
CT	−71.3	−70.5	0.8
MIX	−87.0	−87.4	−0.4

H_3N	CH_3^+	Staggered	Eclipsed	Difference
$2a_1$ and $3a_1$	$2a_1$	173.8	173.8	−0.0
1e	1e	47.6	51.5	3.9

TABLE X. Energy Decomposition of the Rotational Barrier in kcal/mol for H_3B–CH_3^- Using an STO-3G Basis Set

	Staggered	Eclipsed	Difference
ΔE	−170.4	−165.3	5.0
ES	−148.4	−148.5	−0.1
EX	133.9	138.1	4.2
(Overlap)	(263.3)	(270.3)	(7.0)
$(-\sum K)$	(−129.4)	(−132.2)	(−2.8)
PL	−12.0	−12.0	0.0
CT	−43.3	−42.1	1.3
MIX	−100.5	−100.9	−0.4

H_3B	CH_3^-	Staggered	Eclipsed	Difference
$2a_1$	$2a_1$ and $3a_1$	158.9	159.1	0.2
1e	1e	38.4	45.4	7.0

Thus, from the results for H_3N–BH_3, H_3C–CH_3, H_3Si–SiH_3, H_3C–SiH_3, H_3N–CH_3^+, and H_3B–CH_3^-, it can be concluded that the internal rotation barrier of an H_3X–YH_3 molecule is quantitatively attributable to the pseudo π MO's interactions between the opposite parts, –XH and –YH, of the molecule.

Conclusion

1. MO energy decomposition showed which MO–MO interactions are significant for CT of borazane complex. The order was

$$CT_{H_3N,\,3a_1\to BH_3,\,3a_1} > CT_{H_3N,\,3a_1\to BH_3,\,5a_1} > CT_{H_3N,\,5a_1\leftarrow BH_3,\,2a_1} > CT_{H_3N,\,2e\leftarrow BH_3,\,1e}.$$

2. In the intermolecular overlap repulsion of borazane, the order in the valence MO's was

$$EX'_{H_3N,\,3a_1-BH_3,\,2a_1} > EX'_{H_3N,\,2a_1-BH_3,\,2a_1} > EX'_{H_3N,\,1e-BH_3,\,1e}$$

The overlap repulsion between the core MO of BH_3 and the valence MO's of NH_3 could not be neglected.

3. The internal rotation barrier of borazane originates from the overlap repulsion between 1e MO's of NH_3 and of BH_3.

4. The origin of the internal rotation barrier of ethane is also attributable to 1e MO's interactions.

5. From the results for H_3N–BH_3, H_3C–CH_3, H_3Si–SiH_3, H_3C–SiH_3, H_3N–CH_3^-, and H_3B–CH_3^+, the internal rotation barrier of an H_3X–YH_3 molecule is attributable to the pseudo π MO's interactions between –XH and –YH bonds of the molecule.

Acknowledgement The authors are grateful to Professor Tsuboi of Tokyo University for helpful and stimulating discussions.